

Research Article

Pathway to Multi-Response Characterization of the Improved Elliptical Vessel Solar Receiver for Efficiencies Maximization

Thomas Okechukwu Onah^{*} , Christian Chikezie Aka ,
Onyekachi Marcel Egwuagu 

Department of Mechanical and Production Engineering, Enugu State University of Science and Technology Enugu, Enugu, Nigeria

Abstract

Studies on the pathway to multi-response characterization of the improved elliptical vessel solar receiver for environmental sustainability has been studied. The materials were sourced based on categories of components element: support mechanisms made of mild steel plates, bolts, nuts, clamps, and water as heat transfer fluid. The reflector was made of aluminum foil tape while the vessel has a glass cover fitted with bolts and nuts, the receiver is made of copper pipe, aluminum pipe, galvanized iron pipes, and stainless steel pipes. They are fitted into the vessel with chlorinated polyvinyl chloride 3/4 pipes, and journal-bearing mechanisms. Furthermore, glass cover attachment reduces radiative heat loss coefficient by eliminating wind influence and increases heat flux inside the vessel thereby improving heat transfer, hence improving the overall system's efficiency. The pathway to multi-response characterization showed that the average experimental thermal efficiency rose from 9.83% to 12.55% and from 4.42% to 7.03% for Polyurethane coated Copper and Aluminum respectively. It reduced from 9.83% to 8.53% and from 8.10% to 6.50% respectively for Polyurethane coated Galvanized Iron and Aluminum. This depicts the gleam appearance of Polyurethane coating on Galvanized Iron and stainless steel thus reducing their heat absorption coefficient and in turn reducing their efficiency.

Keywords

Solar, Efficiencies, Vessel, Receiver, Heat

1. Introduction

The prompt global growth in population has led to a high energy mandate, especially in developing countries like Nigeria. These nations are confronted with the challenges of breeding, storing, when not needed and sufficiently contributing clean, maintainable energy to their citizens. Presently, some chief energy production sources practice environmental

pollutants, such as fossil fuels, nuclear fuels, etc [1, 2]. The commutative energy prerequisite, apprehension for the environment, and accordingly its values are anticipated to rise. The creation of acceptable and environmentally friendly alternative energy sources is a straightforward way to address these challenges [3]. In addition, it is projected that uncon-

^{*}Corresponding author: okechukwu.onah@esut.edu.ng (Thomas Okechukwu Onah)

Received: 5 April 2024; Accepted: 22 April 2024; Published: 17 May 2024



Copyright: © The Author(s), 2024. Published by Science Publishing Group. This is an **Open Access** article, distributed under the terms of the Creative Commons Attribution 4.0 License (<http://creativecommons.org/licenses/by/4.0/>), which permits unrestricted use, distribution and reproduction in any medium, provided the original work is properly cited.

ventional energy sources like solar energy will soon become very important to the energy supply. In the future, renewable resources will play a vital role as the world's demand for energy rises and traditional energy sources like coal and petroleum become less abundant. The Elliptical Vessel Receiver (EVR) is primarily used in steam power plants to generate electricity because it can supply thermal energy up to 400 °C. Enugu state and most northern states of Nigeria have the potential to host a well-known EVR solar energy application.

There is a critical energy emergency that the entire world is currently experiencing. The foundation of every human action on earth is energy. Energy resources are inadequate, despite an increase in energy demand. These resources will run out if fuel and energy consumption continue at their current rate for the next 20 to 40 years. Humans have become reliant on energy, which has impelled the development of alternative energy sources, such as solar energy, wind energy,

and tidal energy. It is relatively expensive to operate solar energy notwithstanding its profusion. Efforts are being made to develop solar-powered systems that are economical, reliable, and robust.

As a free, renewable, and environmentally friendly energy source, solar energy is also found everywhere in the world. Solar photovoltaic and solar thermal systems are the two methods for garnering solar energy. A variety of technologies, including flat plate collectors (FPC), concentrated solar power systems (CSP), and evacuated tube collectors (ETC), have been utilized as solar thermal systems to harvest energy. In addition, CSP systems can be further divided into compound parabolic collectors (CPC), solar towers, solar EVR, linear Fresnel collectors, parabolic trough collectors (PTC), and solar parabolic dish concentrators. Figure 1 depicts different kinds of CSP systems.

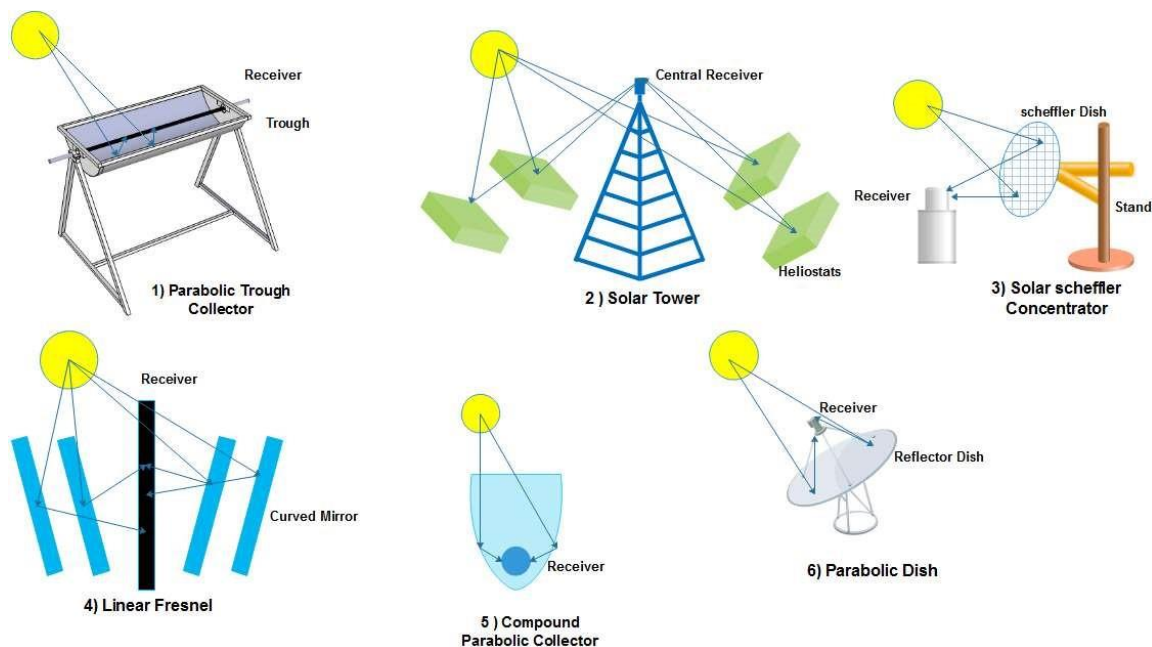


Figure 1. Types of Concentrated Solar Power Systems [3].

EVR is a collector that focuses on lines irradiation. A reflector inside the elliptical vessel directs solar beams in the direction of the receiver. A vessel transfers heat energy while continuously tracking the sun. Heat transfer fluid (HTF) transfers heat energy from the absorber through heat exchange by passing through it. This absorbed heat is used in many applications. It is noted that the ratio of concentration of EVR is greater than 10 according to [4]. It has a variety of applications as well as different areas of installation like roof top and on ground.

Power plants using solar thermal energy that run over 800 degree Celsius are called solar turrets or heliostats. Around a solar tower is an array of mirrors called heliostats. In the direction of the central receiver, which is situated above the

summit of the tower, heliostat mirrors are concentrated on the sun beam. Through the mirrors, reflecting solar rays, are tracked continuously. One disadvantage of this system is that it needs a large space for operation.

Its ratio of concentration is roughly 1000. Therefore, the capacity of all CSP plants worldwide was approximately 1 GW in 2010. By 2030 and 2050, respectively, that amount is likely to increase by 7% and 25%. [5]. Reddy and Kumar (2012) examined electricity generation using water and oil as heat transfer fluids. This calls for the pathway to multi-response characterization of the improved elliptical vessel solar receiver for efficiencies maximization.

2. Methodology

Four dissimilar receivers was used in the analysis. Copper, Stainless Steel, Aluminum, and Galvanized Iron (G. I) pipes with 20 mm external diameter and 88 mm length was used as receivers. The pipes ends are fixed with a union joint made of (¾) chlorinated polyvinyl chloride (CPVC) for smooth connections. The other twelve pipes with same material and dimensions were each four coated with turmeric, polyurethane and shred tyre. 8 mm thickness expanded polyethylene

(EPE) sheet is used as insulation material. Figures 2 and 3 show the uncoated receivers and the coating materials respectively. With the EPE sheet insulation, water storage tanks and connector pipes are well-insulated. At different system components, temperature is measured using thermocouples looped to a central digital panel. For monitoring the temperature of the HTF's intake and output, a unique setup is needed. The insulation material and the thermocouples are shown in Figure 4 (A) and (B) respectively.



Figure 2. Receiver Materials.



Figure 3. Coating Materials.

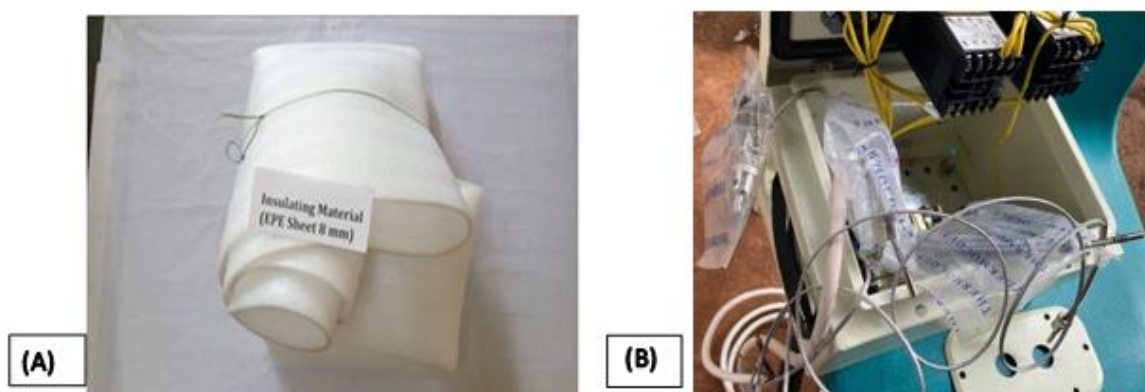


Figure 4. (A) Insulation Material and (B) 5M K-Type Thermocouple 100mm Sensor Probe Temperature from -100 °C to 1250 °C.

An aluminum foil tape reflector was used which gave the best reflective quality as well as a higher intercept factor as tested by [6]. There are many different thicknesses of aluminum foil tape, including 48 mm and 72 mm, as well as lengths of 20 meters which are early obtainable from the local market at low and affordable prices. The aluminum foil was adhered 0.5 mm thick G. I. sheet and stuck to an enclosure made of mild steel that forms the Solar Vessel. At the Standard Organization of Nigeria (SON), Abuja, the reflectivity of the reflector is tested. Figure 5 shows the aluminum foil tape reflector sheets.

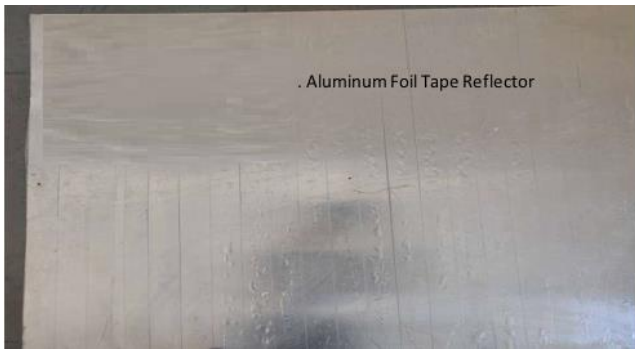


Figure 5. Aluminum Foil Reflector.

Temperatures at various places in the system are measured and recorded using a thermocouple and a panel for reading the thermocouple. The thermocouples were lopped to the panel as well. The wind speed is measured using a Uni-T digital anemometer (UT363). Recorded data read from the panel and recorded in the laptop. Solar radiation is measured using Solar Power Meter (SM206-SOLAR) and is gauged in W/m^2 . Figure 6 displayed the measurement tools. However experimental results are impacted by instrumental error and result uncertainty and ambiguity [7]. Klein recommends methods to find experiment uncertainty which is applied on sourced materials and instrumentations.



Figure 6. Equipment used for measurement.

2.1. Experimental Thermal Efficiency

Two approaches to determine thermal efficiency: theoretically and experimentally. Since the analysis of experiments is the main focus of this work, the following equation is used to calculate the experimental thermal efficiency [8, 9] as in Equation. (1). This is also made possible by design modification of elliptical solar receiver by response surface methodology which optimized the intercept factor by 32.2% according to

$$\eta_{thexp} = \frac{\text{Useful Energy}}{\text{Available Energy}} = \frac{Q_{eu}}{Q_{ea}} = \frac{Q_{eu exp}}{I_{rb} \cdot A_a} \quad (1)$$

Where $Q_{eu exp}$ is the Experimental useful heat energy in Watt (W) as given in Equation. (2).

$$Q_{eu exp} = M \cdot C_p \cdot \Delta T \quad (2)$$

$$\text{But } \Delta T = (T_o - T_i)$$

Where M is the mass flow rate of water in kilogram per hour (kg/hr), C_p Specific heat of water in ($J \cdot kg^{-1} \cdot K^{-1}$), and T_o , T_i is the outlet and inlet water temperature in K.

And Available Energy at the receiver in the form of solar heat flux as in Equation. (3)

$$Q_{ea} = I_{rb} \cdot A_a \quad (3)$$

Where, I_{rb} Is the Beam (direct) radiation in Weber per meter square (W/m^2) and A_a is the aperture area in meter square m^2 .

2.2. Optical Theoretical Efficiency

The overall theoretical efficiency of the ELLIPTICAL VESSEL RECEIVER system is mostly determined by optical efficiency. Optical efficiency is crucial in determining if the system is flawless. Equation (4) gives the formula for calculating optical theoretical efficiency. [10-12], (4)

$$\eta_{opt theo} = \alpha \cdot \rho_m \cdot \gamma \cdot K \quad (4)$$

Where, α absorption coefficient of receiver and ρ_m reflectivity of the reflector, are material properties, γ is the intercept factor and K is equal to 1 when tracking is provided. The following equation (5) can be used to get the intercept factor γ . As experimented and reported by [9]

$$\gamma = \frac{\int_A^B I(w) dw}{\int_{-\infty}^{+\infty} I(w) dw} \quad (5)$$

Where $I(w)$ denotes the reflected radiations, A and B denote a range corresponding to the receiver's outer diameter as shown in Table 1

2.3. Theoretical Thermal Heat Loss

The convective heat transfer coefficient (h_w) and the radiative heat transfer coefficient ($h_{r,r-a}$) are summed to generate theoretical thermal heat loss (U_{Lth}). Wind can lower the amount of convection heat transfer between a receiver and the surrounding air. It can be determined by the following equation [8, 9, 13, 12] see Equation. (6)

$$h_w = \frac{N_{ua} \cdot k_a}{D_{r.ext}} \quad (6)$$

Where $D_{r.ext}$ is the receiver external diameter, k_a is the conductivity of air and N_{ua} represents Nusselt number of air and can be determined by the following equations, as in Equations. (7 and 8)

$$N_{ua} = 0.4 + 0.54 \cdot Re_a^{0.53} \text{ For } 0.1 < Re_a < 1000 \quad (7)$$

$$N_{ua} = 0.3 \cdot Re_a^{0.6} \text{ For } 1000 < Re_a < 50,000 \quad (8)$$

Where Reynolds number of air Re_a can be calculated by the following equation. (9)

$$Re_a = \frac{V \cdot D_{r.ext}}{\nu_a} \quad (9)$$

Where V is the Wind velocity in m/s and ν_a is the kinematic viscosity in m^2/s .

And the radiative heat transfer coefficient can be found with Equation. (10)

$$h_{r,r-a} = \varepsilon \cdot \sigma \cdot (T_r + T_a) \cdot (T_r^2 + T_a^2) \quad (10)$$

Where ε Thermal emittance, σ is Stefan-Boltzmann constant ($5.6697 \times 10^{-8} \text{ W/(m}^2 \text{ K}^4)$), and T_r, T_a is the Surface temperature of receiver and Ambient temperature respectively in ($^{\circ}\text{C}$)

The overall heat loss coefficient can be found by the summation of equation (11) and equation (12) as shown in Equation. (13)

$$U_{Lth} = h_w + h_{r,r-a} \quad (11)$$

2.4. Theoretical Efficiency

Theoretical efficiency can be found by the following equation [8, 13] as shown in Equation. (12)

$$\eta_{theo} = \eta_{opt theo} - \frac{U_{Lth} \cdot A_r \cdot (T_r - T_a)}{I_b \cdot A_a} \quad (12)$$

2.5. Beam Radiation

Direct solar radiation is transformed into usable thermal energy by concentrating solar collectors. A digital solar power meter that tracks total solar radiation is used to measure solar radiation. Hottel model is used to forecast beam radiation from total radiation. [9, 14, 15] as in Equation. (13)

$$a_0 = 0.2538 - 0.0063 (6 - A)^2$$

$$a_1 = 0.7678 + 0.0010 (6.5 - A)^2$$

$$k_1 = 0.249 + 0.081 (2.5 - A)^2$$

$$I_b = I_o (a_0 + a_1 \times e^{-\frac{k_1}{\cos \theta_z}}) \quad (13)$$

Where A' is an altitude of Akwuke = 108 m = 0.108 km and θ_z is the zenith angle. I_o is the total radiation, a_1, a_0 and k_1 are constants which are functions only of altitude and of haze model (visibility range) [16].

3. Results and Discussions

The pathway to multi-response characterization of the improved elliptical vessel solar receiver for efficiencies maximization a better context were chosen to achieve greater efficiency. The combination of intercept factor of 0.341 and receiver absorptivity coefficient value of 0.98 is the best-fitted pair in Table 1 as a solution. The highest efficiency is delivered by the aluminum foil reflector and copper receiver with shred tyre carbon coating, giving $\eta_{thexp} = 19.86\%$ and $\eta_{theo} = 23.19\%$. The efficiency results are equitably consistent with [17-19].

Table 1. Result of Response Optimization for η_{theo}, η_{exp}

Response Optimization for $\eta_{theo}, \eta_{thexp}$					
	Intercept Factor	Receiver (α)	η_{theo} Fit	η_{thexp} Fit	Composite Desirability
Old Design [6]	0.231	0.98	15.28	12.38	0.98
Improved Design	0.341	0.98	23.19	19.86	0.98
% Response Optimization	32.2	0	8.19	7.47	0

The given equations were used to compute the experimental, optical, and theoretical efficiencies. Experimentally, determining optical efficiency is exceedingly challenging. It is challenging to match the co-relation between practical and theoretical efficiency since optical efficiency is frequently evaluated using numerical methods. Here efforts were made to calculate all the efficiencies with experimental data and it was found that variation in efficiencies values of the experimental and theoretical are within a difference of 5% while there is no significant variation in efficiencies value of the optical and theoretical efficiency. It was established from the response optimization that the intercept factor was improved by 32.2%. Similarly, the theoretical efficiency was improved by 8.19% while the experimental thermal efficiency was improved by 7.47%.

Figures 7, 8, 9, and 10 depict the efficiencies calculated

utilizing aluminum foil reflectors and the various receivers: coated and uncoated with different coating materials. The coatings increase the experimental efficiency of the receivers. It is shown that the efficiency was highest with 19.37% for experimental efficiency, 23.20% for optical theoretical efficiency and 23.19% for theoretical efficiency with Shred Tyre coating followed by Turmeric 14.08 %, 15.86% and 15.85% for these efficiencies. Dissimilarity, there is a decrease on the experimental thermal efficiency, optical theoretical efficiency as well as theoretical efficiency of G. I and S. S coated Polyurethane except for Cu and AL coated Polyurethane that show a little increase. This is due to the high absorptivity value of uncoated G. I and S. S, the absorptivity has been affected by polyurethane coating on these materials. Among the four absorbers when uncoated, the efficiencies increase in order of Al - S. S - Cu - G. I.

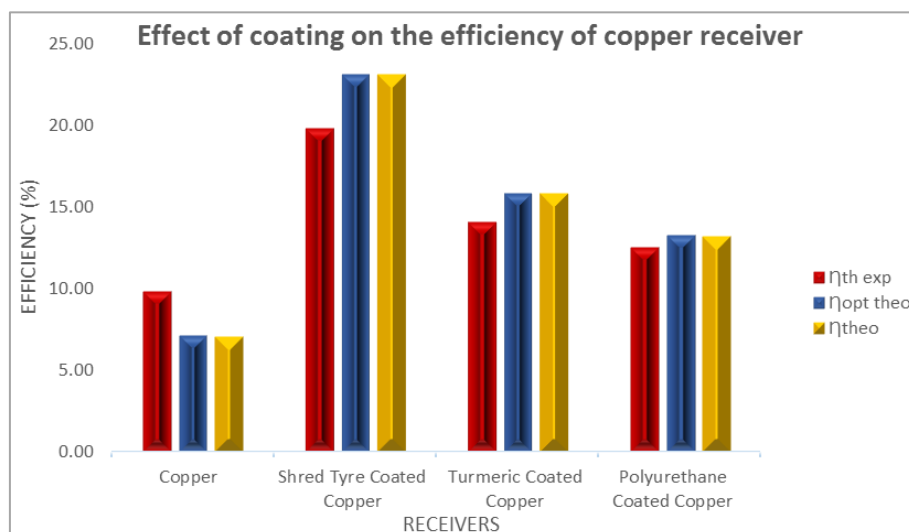


Figure 7. Average Efficiency Plot of Copper Receiver.

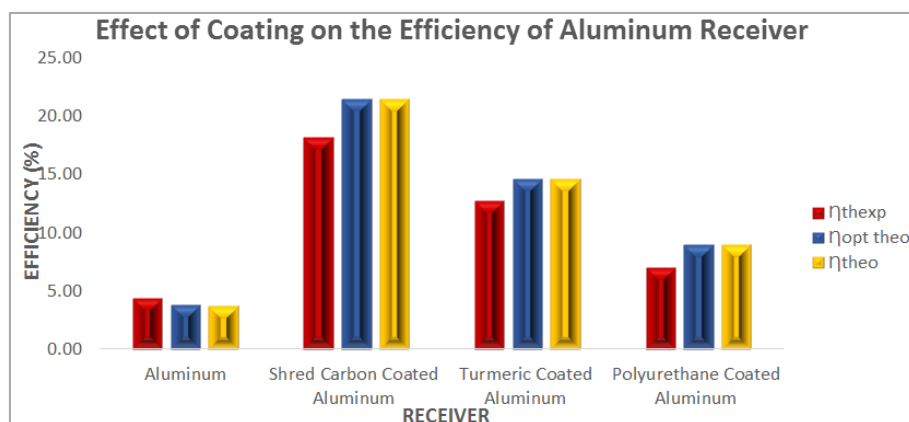


Figure 8. Average Efficiency Plot of Aluminum Receiver.

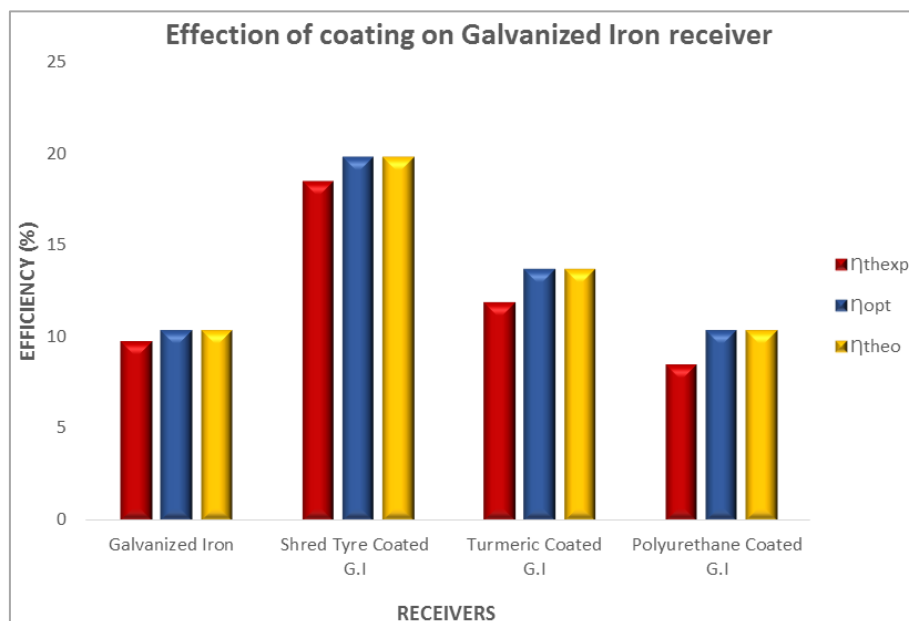


Figure 9. Average Efficiency Plot of Galvanized Iron Receiver.

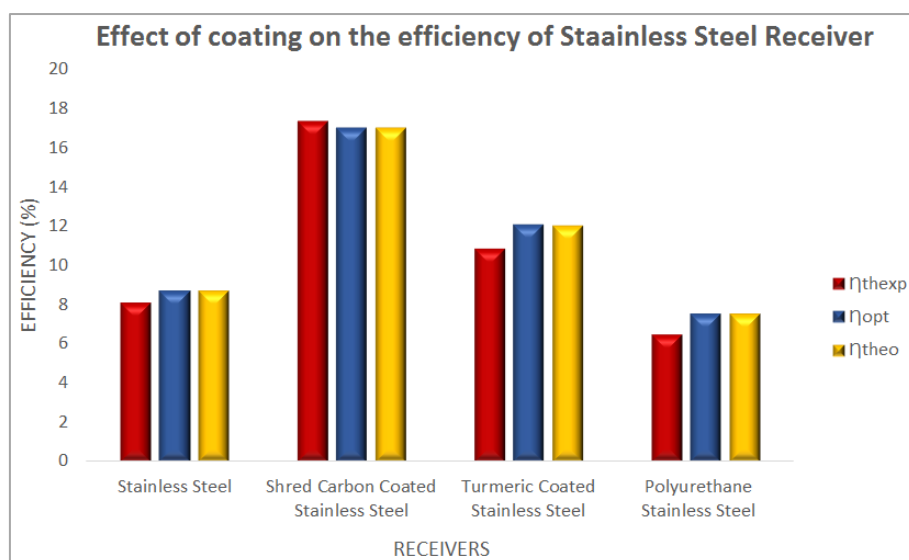


Figure 10. Average Efficiency Plot of Stainless Steel Receiver.

However Figure 11 showed that Polyurethane coating has much positive influence on the efficiency on its coating on Cu and Al with a negative influence on the efficiency of its coating on G. I and S. S. The theoretical efficiency of Cu with ST increases in the order from SS - G. I - Al - Cu while the theoretical efficiency of Tu and Pe coating increases in the order from SS - Al - G. I - Cu for all the different coating combinations. Overall, coating with ST which is a near perfect black body has the highest efficiency followed by Tu coating, whereas Pe coating had the lowest. The pair of ST coating and Cu receiver had the highest experimental and

theoretical efficiency 19.37% and 23.19% respectively. In addition, the theoretical efficiency of the pair ST + Al came second and ST+G. I came third whereas the experimental efficiency of ST + G. I was second followed ST + Al and pair ST + SS has the lowest experimental and theoretical efficiency 17.34% and 17.02% respectively, It was also noted that, the experimental efficiency of Cu and G. I are almost same when they are not coated whereas the experimental efficiency of Tu coated Al is also higher than the experimental efficiency of Tu coated G. I.

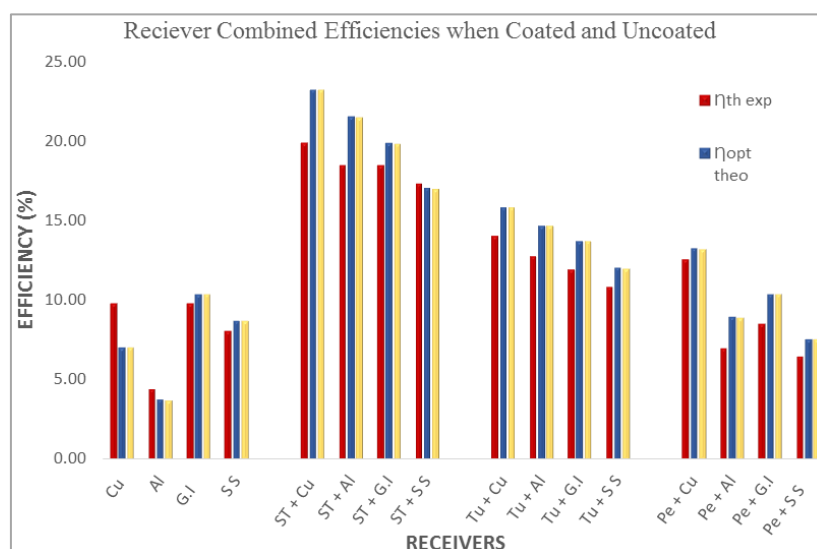


Figure 11. Efficiency Plot for Coated and Uncoated Receivers.

4. Conclusion

It was established from the response optimization that the intercept factor was improved by 32.2%. Similarly, the theoretical efficiency was improved by 8.19% while the experimental thermal efficiency was improved by 7.47%. The highest experimental thermal efficiency of 21.31%, and outlet temperature difference of 16.95 °C were recorded between 13:10 hrs. to 14:10 hrs. Thus use of glass cover attachment has eliminated the influence of wind speed and also increases the heat flux inside the vessel thereby improving heat transfer. Furthermore, the receiver's ability to absorb heat is improved by a black shred tyre coating, this also improves the overall system's efficiency. These shows that Cu and Shred tyre coating allows for the highest thermal energy transfer than other receiver and coating combinations and therefore more efficient.

Author Contributions

Thomas Okechukwu Onah: Conceptualization, Resources

Christian Chikezie Aka: Data curation, Methodology

Onyekachi Marcel Onyekachi: Formal Analysis, Investigation

Funding

This research received no specific grant from any funding agency in the public, commercial, or not-for-profit sectors.

Data Availability Statement

The data that support the findings of this study are available on request from the corresponding author.

Conflicts of Interest

The authors declare that there is no conflict of interest.

References

- [1] A. D. Ramirez, B. Rivela, A. Boero, A. M. Melendres, A. D. Ramirez and B. Rivela, "Lights and shadows of the environmental impacts of fossil-based electricity generation technologies: A contribution based on the Ecuadorian experience," *Energy Policy*, vol. 125, p. 467–477, 2019.
- [2] M. Lodhi, A. Z. Abidin, M. Yusof Sulaiman, M. Lodhi, A. Z. Abidin and M. Yusof Sulaiman, "Pollutant emissions from fossil fuel use in Kuala Lumpur and environmental damage," *Energy Conversion and Management*, vol. 38, no. 3, p. 213–216, 1997.
- [3] M. Shahzad, Y. Qu, S. A. Javed, A. U. Zafar, S. U. Rehman and M. Shahzad, "Relation of environment sustainability to CSR and green innovation: A case of Pakistani manufacturing industry," *Journal of Cleaner Production*, vol. 253, pp. 119–938, 2020.
- [4] C. C. Aka, T. O. Onah. & O. M. Egbuagu, "Design modification of elliptical vessel solar receiver by response surface methodology," *Global Journal of Engineering and Technology Advances*, vol. 19, no. 01, p. 129–142, 2024.
- [5] A. Ummadisingu and M. Soni, "Concentrating solar power – Technology, potential and policy in India," *Renewable and Sustainable Energy Reviews*, vol. 15, no. 9, p. 5169–5175, 2011.

- [6] B. H. Upadhyay, A. J. Patel, P. V. Ramana, B. H. Upadhyay, A. J. Patel and P. V. Ramana, "Parabolic Trough Collector, a Novel Design for Domestic Water Heating Application," *IJRASET*, vol. 5, no. X, p. 497–503, 2023.
- [7] T. Force, "Uncertainty of Experimental Data," *Lecture Notes*, pp. 1-9, 2003.
- [8] Sagade, N. Shinde, P. & Patil, M. A. Sagade, N. Shinde and P. & Patil, "Effect of Receiver Temperature on Performance Evaluation of Silver Coated Selective Surface Compound Parabolic Reflector with Top Glass Cover," *Energy Procedia*, vol. 48, p. 212–222, 2014.
- [9] J. A. Duffie, W. A. Beckman, W. M. Worek, J. A. Duffie, A. Beckman W. and W. M. Worek, "Solar Engineering of Thermal Processes," 2018.
- [10] A. K. Hussein, "Applications of nanotechnology to improve the performance of solar collectors – Recent advances and overview," *Renewable and Sustainable Energy Reviews*, vol. 62, p. 767–792, 2016.
- [11] Y. Wang, J. Xu, Q. Liu, Y. Chen, H. Liu and Y. Wang, "Performance analysis of a parabolic trough solar collector using Al_2O_3 /synthetic oil nanofluid," *Applied Thermal Engineering*, vol. 107, p. 469–478, 2016.
- [12] T. A. Yassen, "Experimental and Theoretical Study of a Parabolic Trough Solar," *Anbar Journal of Engineering Sciences*, vol. 5, no. 1, p. 109–125, 2012.
- [13] M. Ghodbane and B. Boumeddane, "Optical Modeling and Thermal Behavior of a Parabolic Trough Solar Collector in the Algerian Sahara," *Modelling, Measurement & Control*, vol. 86, no. 2, p. 406–426, 2017.
- [14] H. C. Hottel, "A simple model for estimating the transmittance of direct solar radiation through clear atmospheres," *Solar Energy*, vol. 18, no. 2, p. 129–134, 1976.
- [15] A. A. Sagade and N. N. Shinde, "Performance evaluation of parabolic dish type solar collector for industrial heating application," *International Journal of Energy Technology and Policy*, vol. 8, no. 1, p. 80, 2012.
- [16] S. A. Sadat, B. Hoex, J. M. Pearce, S. A. Sadat, B. Hoex and J. M. Pearce, "A review of the effects of haze on solar photovoltaic performance," *Renewable & Sustainable Energy Reviews*, vol. 167, p. 112796, 2022.
- [17] A. Bharti, A. K. Mishra, B. Paul, A. Bharti, A. K. Mishra and B. Paul, "Thermal performance analysis of small-sized solar parabolic trough collector using secondary reflectors," *International Journal of Sustainable Energy*, vol. 38, no. 10, p. 1002–1022, 2019.
- [18] D. Kumar and S. Kumar, "Thermal performance of the solar parabolic trough collector at different flow rates: an experimental study," *International Journal of Ambient Energy*, vol. 39, no. 1, p. 93–102, 2022.
- [19] B. H. Upadhyay, A. J. Patel, P. V. Ramana, B. H. Upadhyay, A. J. Patel and P. V. & Ramana, "Comparative study of parabolic trough collector for low-temperature water heating," *Energy Sources, Part A: Recovery, Utilization, and Environmental Effects*, p. 1–17, 2023.